

■ Electro, Physical & Theoretical Chemistry

Organomagnesium Crown Ethers and Their Binding Affinities with Li^+ , Na^+ , K^+ , Be^{2+} , Mg^{2+} , and Ca^{2+} Ions – A Theoretical Study

Saikat Roy,^[a] Krishnan Thirumoorthy,^[b] Uday Kumar Padidela,^[c] Pothiappan Vairaprakash,^[d] Anakuthil Anoop,^{*[a]} and Venkatesan S. Thimmakonda^{*[e]}

Novel organomagnesium crown ether molecules have been computationally characterized using density functional theory (DFT). Monomer units of MgC_6 are used as building blocks. Isomers of MgC_6H_2 have been extensively explored using both DFT and coupled-cluster methods in the past by some of us. It had been concluded that the seven-membered ring isomer, 1-magnesiumcyclohept-4-en-2,6-diyne, was the thermodynamically most stable molecule at all levels. Thus, the latter has been used as the building block for designing new organomagne-

sium crown ethers. Both alkali (Li^+ , Na^+ , and K^+) and alkaline-earth (Be^{2+} , Mg^{2+} , and Ca^{2+}) metal ions selective complexes have been theoretically identified. Theoretical binding energies (ΔE at 0 K) and thermally corrected Gibbs free energies (ΔG at 298.15 K) have been computed for these molecules with MgC_6 -6-crown-2, MgC_6 -9-crown-3, and MgC_6 -12-crown-4 hosts. Higher binding affinity values obtained for Be^{2+} indicate that these new crown ether molecules could effectively be used for Be^{2+} encapsulation.

Introduction

More than 10,000 crown ether molecules have been reported to date^[1–5] since the original discovery of crown ethers accidentally happened in 1967 by Pedersen.^[6–7] However, the concept of crown ethers remains fascinating due to the potential applications of these molecules in various fields including (but not limited to) phase transfer catalysis,^[8] ion-sensing,^[9,10] nuclear waste management,^[11–13] and analytical methods.^[14] The ability of crown ethers to recognize and trap different metal ions depending on the size of the macrocyclic

ring, type of the donor atom (N, O, and S and thus hard-soft interactions), and polarity of the medium strengthened their utility in various aspects.^[15–20]

Various isomers of MgC_6H_2 have been extensively explored by Thimmakonda and co-workers, in a previous theoretical study, using density functional theory (DFT) and coupled-cluster methods.^[21] The thermodynamically most stable isomer for MgC_6H_2 was identified to be 1-magnesiumcyclohept-4-en-2,6-diyne. Theoretical studies carried out by Largo and co-workers at the B3LYP/6-311G(d) and B3LYP/6-311+G(d) level of theories on bare MgC_6 elemental composition concluded that the singlet electronic state of the cyclic isomer is the most stable molecule.^[22] Therefore, utilizing the cyclic MgC_6 as a base unit in building the new crown ether molecules is justified beyond any reasonable doubts. Here, we have computationally designed four different organomagnesium crown ethers (MgC_6 -6-crown-2, MgC_6 -9-crown-3, and MgC_6 -12-crown-4 (two different isomers)) using MgC_6 as a base unit (see Figure 1).

Optimized geometries of these molecules in the ball and stick model including energy differences in case of multiple structural isomers (MgC_6 -12-crown-4) are shown in Figure 2. The IUPAC names are given in Table 1. These IUPAC names have been cross checked with the Cambridge OPSIN software.^[23] At the moment, pentamers and hexamers have not been considered in this study due to the computational viability of performing the calculations as well as the multiple number of structural isomers possible in these two cases.

We have computed gas phase binding affinities of these crown ether molecules with alkali (Li^+ , Na^+ , and K^+) and alkaline-earth (Be^{2+} , Mg^{2+} , and Ca^{2+}) metal ions (see Tables 2 and 3). The binding affinities have been explicitly studied at five different level of theories each for MgC_6 -6C2, MgC_6 -12C3, and MgC_6 -12C4. The solvent effects are not considered in this

[a] S. Roy, Prof. A. Anoop
Department of Chemistry,
Indian Institute of Technology Kharagpur,
Kharagpur 721 302, West Bengal, India
E-mail: anoop@chem.iitkgp.ac.in

[b] Dr. K. Thirumoorthy
Department of Chemistry,
School of Advanced Sciences,
Vellore Institute of Technology,
Vellore - 632 014, Tamil Nadu, India

[c] Dr. U. K. Padidela
Department of Chemistry,
Birla Institute of Technology and Science,
Pilani, K K Birla Goa Campus, Goa - 403 726, India

[d] Dr. P. Vairaprakash
Department of Chemistry,
School of Chemical and Biotechnology,
SASTRA Deemed University,
Thanjavur – 613 401, Tamil Nadu, India

[e] Dr. V. S. Thimmakonda
Department of Chemistry and Biochemistry,
San Diego State University,
San Diego, CA 92182-1030, USA
E-mail: vthimmakondusamy@sdsu.edu

Supporting information for this article is available on the WWW under <https://doi.org/10.1002/slct.202102317>

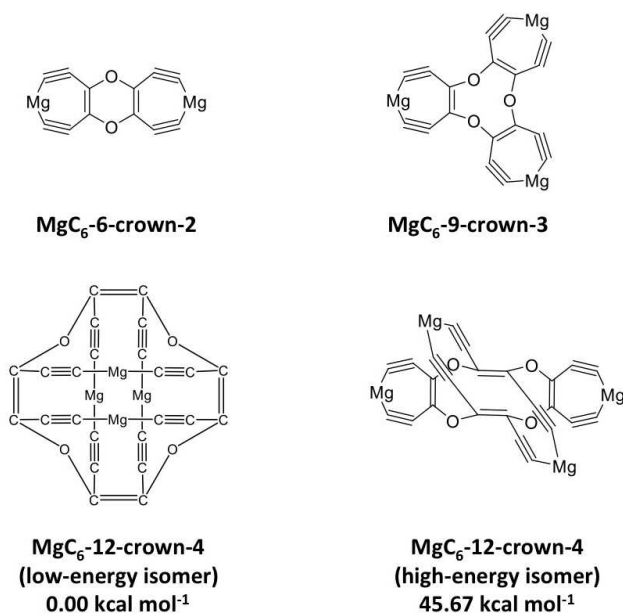


Figure 1. Organomagnesium crown ethers theoretically identified. ZPVE-corrected relative energies are obtained at the B3LYP-D3BJ/6-311++G(2d,2p) level of theory.

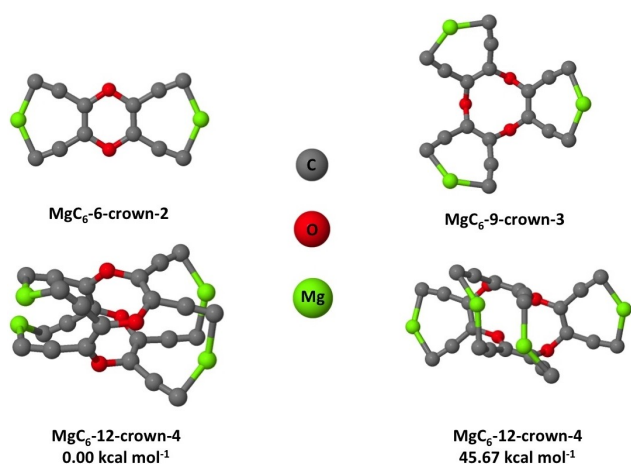


Figure 2. Optimized structures of organomagnesium crown ethers identified at the B3LYP-D3BJ/6-311++G(2d,2p) level of theory.

study as the current investigation predominantly focused on the intrinsic binding affinities within the gas-phase to thoroughly understand the molecular recognition of these new host molecules. It is noted here that ligand exchange processes on solvated beryllium cations are discussed elsewhere in the literature.^[24]

The results showed a selective binding of Li⁺ among alkali metal ions and Be²⁺ among the alkaline-earth metal ions. This observation is highly relevant for the following reasons. The separation of Li⁺ from Mg²⁺ ion remains as a challenge even to date.^[25] Thus, designing new ligands, which could effectively bind one ion over the other is a key problem to address. Though toxic, beryllium and its alloys are indispensable for the aeronautic and space industry^[26,27] due to their comparable mechanical properties to steel but non-magnetic and non-sparking. However, one of the major safety issues in using beryllium and its compounds is that they can cause the development of chronic beryllium disease.^[28–30] For this reason, beryllium chemistry is somewhat underdeveloped from an experimental perspective.^[31–33] Thus, computational designing of new ligands which could effectively bind with Li⁺ and Be²⁺ ions are important before extensive experimental efforts in finding a suitable host molecule. Perhaps, we leave this discussion with a caveat that experimental studies on various beryllium crown ether molecules were carried out in the groups of Dehnicke,^[34,35] Puchta,^[36] and Buchner.^[37,38]

Computational Details

Geometry optimization and frequency calculations have been done using DFT with the hybrid-functional B3LYP^[39–41] and the 6-311++G(2d,2p) basis set.^[42,43] All stationary points obtained at this level have been reoptimized including Grimme's empirical dispersion corrections (D3)^[44] with Becke-Johnson damping (D3BJ)^[45,46] to account for the dispersion (i.e., van der Waals) interactions.^[47] Further, all geometries have been optimized with the TPSSH^[48] hybrid-meta functional first without and later with D3BJ corrections. Truhlar's M06-2X^[49] hybrid-meta functional has also been used. As this functional already incorporates certain amount of dispersion correction within, additional D3BJ corrections on top of this functional have not been required. All the organomagnesium crown ethers studied here are found to be minima (i.e., zero imaginary frequencies) at all these five different level of theories. For all host molecules, ab initio molecular dynamics (AIMD) simulations using the atom-centered density matrix propagation (ADMP)^[50] approach have been carried out at the B3LYP/6-31G(d)

Table 1. IUPAC names of MgC₆ crown ethers.

Crown-ether	Name	IUPAC Name
MgC ₆ -6-crown-2	MgC ₆ -6C2	6,14-dimagnesia-2,10-dioxatricyclo[9.5.0.0 ^{3,9}]hexadeca-1(11),3(9)-dien-4,7,12,15-tetraene
MgC ₆ -9-crown-3	MgC ₆ -9C3	6,14,22-trimagnesia-2,10,18-trioxatetracyclo[17.5.0.0 ^{3,9} .0 ^{11,17}]tetracosan-1(19),3(9),11(17)-trien-4,7,12,15,20,23-hexayne
MgC ₆ -12-crown-4	MgC ₆ -12C4 low energy	(1Z,7Z,9Z,15Z)-8,16,24,32-tetraoxa-4,12,20,28-tetramagnesapentacyclo[21.9.0.0 ^{2,17} .0 ^{9,31} .0 ^{15,25}]dotriaconta1(23),7(17),9(31),15(25)-tetraen-2,5,10,13,18,21,26,29-octayne
MgC ₆ -12-crown-4	MgC ₆ -12C4 high energy	7,18,25,30-tetramagnesia-3,11,14,22-tetraoxapentacyclo[11.9.5.5 ^{2,12} .0 ^{4,10} .0 ^{15,21}]dotriacontan-1,4(10),12,15(21)-tetraene-5,8,16,19,23,26,28,31-octayne

Table 2. Binding energies (ΔE ; ZPVE inclusive; in kcal mol⁻¹) and Gibbs free energies (ΔG ; in kcal mol⁻¹) of metal-ion chelated MgC₆-6C2 and MgC₆-9C3 calculated at different levels.^[a]

host MgC ₆ ⁻	ion ΔE	B3LYP		B3LYP-D3BJ		TPSSh		TPSSh-D3BJ		M06-2X	
		ΔG	6-311 + + G(2d,2p) ΔE	ΔG	ΔE	ΔG	ΔE	ΔG	ΔE	ΔG	
6C2	Li ⁺	-43.15	-36.43	-45.64	-39.66	-42.20	-35.98	-43.79	-37.95	-42.27	-36.24
	Na ⁺	-33.03	-26.14	-36.07	-30.29	-32.06	-25.66	-34.01	-28.00	-33.09	-26.82
	K ⁺	-24.73	-18.18	-27.99	-22.84	-24.28	-18.29	-26.42	-22.95	-26.19	-20.13
	Be ²⁺	278.67	-269.43	-283.44	-274.42	-284.20	-275.31	-287.64	-278.91	-266.88	-258.58
Ca ²⁺	Mg ²⁺	164.48	-155.43	-170.10	-161.27	-165.64	-156.89	-169.58	-160.99	-156.08	-148.20
	Ca ²⁺	115.26	-107.43	-121.50	-114.22	-117.34	-109.76	-121.68	-114.53	-113.63	-106.00
9C3	Li ⁺	-64.95	-57.40	-68.34	-60.87	-64.21	-56.65	-66.55	-59.04	-63.42	-55.91
	Na ⁺	-48.14	-41.41	-52.26	-45.45	-47.65	-40.94	-50.52	-43.75	-48.26	-41.65
	K ⁺	-34.83	-28.42	-38.76	-32.29	-34.97	-28.56	-37.77	-31.34	-36.46	-30.10
	Be ²⁺	-351.16	-343.26	-355.21	-347.20	-351.88	-344.26	-354.61	-346.91	-337.02	-329.73
Mg ²⁺	-215.83	-208.64	-221.59	-214.42	-215.40	-208.40	-219.39	-212.44	-209.87	-202.90	
Ca ²⁺	-152.19	-144.34	-157.60	-149.74	-153.18	-146.21	-157.14	-150.25	-146.49	-139.60	

^[a] ΔE values are calculated at 0 K. Thermally corrected ΔG values are calculated at 298.15 K.**Table 3.** Binding energies (ΔE ; ZPVE inclusive; in kcal mol⁻¹) and Gibbs free energies (ΔG ; in kcal mol⁻¹) of metal-ion chelated organomagnesium crown ethers calculated at different levels.^[a]

host MgC ₆ ⁻	ion ΔE	B3LYP		B3LYP-D3BJ		TPSSh		TPSSh-D3BJ		M06-2X	
		ΔG	6-311 + + G(2d,2p) ΔE	ΔE	ΔG						
12C4 (low)	Li ⁺	-50.25	-43.63	-55.83	-49.11	-50.55	-44.04	-54.37	-47.70	-50.34	-43.74
	Na ⁺	-35.73	-29.06	-42.18	-35.25	-35.44	-28.83	-39.97	-33.13	-36.74	-30.14
	K ⁺	-24.55	-18.20	-30.67	-23.96	-24.73	-18.52	-29.17	-22.62	-27.20	-20.90
	Be ²⁺	-330.03	-323.26	-335.12	-328.48	-331.15	-324.64	-335.28	-328.82	-320.92	-314.37
	Mg ²⁺	-203.27	-196.14	-209.73	-202.71	-201.21	-194.30	-206.18	-199.29	-198.01	-191.06
	Ca ²⁺	-142.94	-135.92	-149.59	-142.67	-142.83	-136.01	-147.84	-141.05	-138.41	-131.53
12C4 (high)	Li ⁺	-60.00	-51.98	-70.50	-62.82	-73.09	-64.00	-81.18	-72.16	-72.71	-63.90
	Na ⁺	-46.78	-38.49	-58.49	-50.12	-48.13	-39.94	-55.88	-47.77	-51.30	-42.90
	K ⁺	-32.08	-23.70	-43.35	-35.03	-33.67	-25.47	-41.05	-32.94	-39.12	-30.37
	Be ²⁺	-364.44	-355.83	-377.57	-368.97	-368.63	-359.73	-377.99	-368.96	-359.62	-351.80
	Mg ²⁺	-244.90	-235.67	-258.96	-249.86	-250.88	-241.71	-260.83	-251.51	-250.35	-241.04
	Ca ²⁺	-184.52	-175.07	-199.00	-189.30	-190.07	-180.87	-199.42	-190.07	-190.32	-180.76

^[a] ΔE values are calculated at 0 K. Thermally corrected ΔG values are calculated at 298.15 K.

level of theory to check the kinetic stability of these molecules. These simulations have been done for 500 fs at 298 K. All electronic structure calculations have been done with the Gaussian program package.^[51] To analyze the nature of interactions between the host molecules and guest ions, energy decomposition analyses (EDA)^[52] were carried out with symmetry-adapted perturbation theory (SAPT)^[53] using psi4^[54] at the SAPT0^[55,56]/def2-TZVP^[57]//B3LYP-D3BJ/6-311 + + G(2d,2p) level unless otherwise specified.

Results and Discussion

The binding energies (ΔE at 0 K) and thermally corrected Gibbs free energies (ΔG at 298.15 K) computed for the metal ions with MgC₆-6C2 and MgC₆-9C3 at different level of theories have been collected in Table 2. Likewise, these values obtained for two different isomers of MgC₆-12C4 at different level of theories are collected in Table 3. They are calculated using the following equation

$$\Delta E = E_{\text{complex}} - (E_{\text{host}} + E_{\text{ion}}) \quad (1)$$

where, E_{complex} is the ZPVE-corrected value of the complex, E_{host} is the ZPVE-corrected value of the host, and E_{ion} is the energy of the ion. Similarly, Gibbs free energy values have been calculated using the corresponding thermally corrected energies. Unless otherwise stated, discussions here below refer to calculations carried out at the B3LYP-D3BJ/6-311 + + G(2d,2p) level of theory.

M⁺²⁺-MgC₆-6C2

The dimer host molecule is quasi-planar with C_{2v} symmetry. Two different binding sites have been identified for this host molecule. In one case, the binding occurs on the side of the O-C-C≡C bond, which is depicted in Figure 3(a). In another case, the binding occurs on top of the O-C-C-O ring, which is shown in Figure 3(b). The quasi planar structure of Li⁺-MgC₆-6C2, where both electrostatic and metal-ion-alkyne interactions are possible (Figure 3(a)), was found to be more stable than the puckered ring structure (Figure 3(b)) by 8.77 kcal mol⁻¹. In the latter, electrostatic interactions between the oxygen atoms and

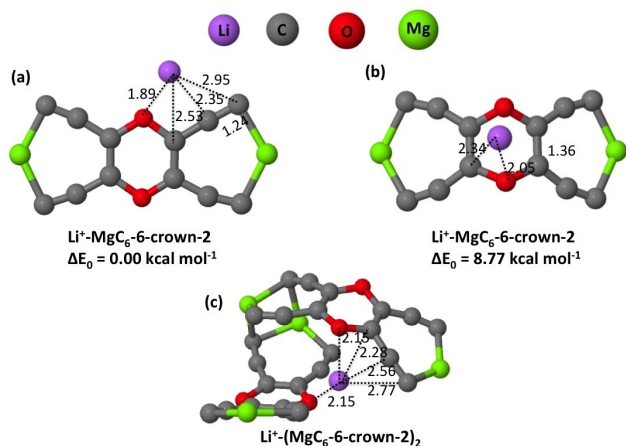


Figure 3. Three different optimized structures of $\text{Li}^+\text{-MgC}_6\text{-6C2}$ identified at the B3LYP-D3BJ/6-311++G(2d,2p) level of theory. (a) binding occurs on the side; (b) binding occurs on top of the O=C=O ring; (c) 2(substrate):1(ion) combination taken. Key bond length parameters are given in $^\circ\text{\AA}$ ngstrom

the metal-ion are possible along with metal-ion-alkene interactions, whereas in the former, electrostatic and metal-ion-alkyne interactions are possible. For this host molecule, the latter combination leads to more stable geometries. For Na^+ , K^+ , Be^{2+} , Mg^{2+} , and $\text{Ca}^{2+}\text{-MgC}_6\text{-6C2}$, where binding occurs on the side, isomers are more stable by 9.78, 8.48, 16.15, 18.74, and 8.66 kcal mol^{-1} , respectively. Therefore, we have calculated the binding energies of all metal ions where the ion binds on the side with the dimer host. For brevity, only the most stable geometries of other metal ions with $\text{MgC}_6\text{-6C2}$ are shown in Figure 4. As per an anonymous reviewer's suggestion, calculations were also done taking two host molecules of the dimer and one metal ion, which is shown in Figure 3(c). The binding

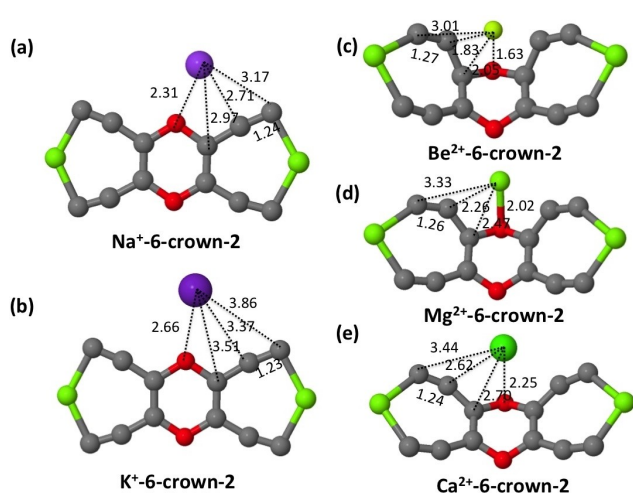


Figure 4. Optimized structures of (a) $\text{Na}^+\text{-MgC}_6\text{-6C2}$; (b) $\text{K}^+\text{-MgC}_6\text{-6C2}$; (c) $\text{Be}^{2+}\text{-MgC}_6\text{-6C2}$; (d) $\text{Mg}^{2+}\text{-MgC}_6\text{-6C2}$, and (e) $\text{Ca}^{2+}\text{-MgC}_6\text{-6C2}$ identified at the B3LYP-D3BJ/6-311++G(2d,2p) level of theory. Key bond length parameters are given in $^\circ\text{\AA}$ ngstrom.

energy and Gibbs free energy obtained for this combination is -40.51 and $-30.02 \text{ kcal mol}^{-1}$, respectively. These values are slightly less compared with the 1(substrate):1(ion) combination (see Table 2). It is noted here that without the presence of Li^+ ion, the host molecule is flat, whose structure is given in the supporting information. More investigation along 2:1 combination for various ions including solvent effects will be carried out in a future study.

The binding energy values calculated for Li^+ are in the range of -42.20 to $-45.64 \text{ kcal mol}^{-1}$ (see Table 2) at different levels. For Na^+ , these values are decreased by $\sim 9\text{--}10 \text{ kcal mol}^{-1}$. For K^+ , the values are further decreased by $\sim 7\text{--}9 \text{ kcal mol}^{-1}$ at all levels. Same observations are true for Gibbs free energies, which are calculated at 298.15 K. Compared to the binding energies, ΔG values are $6\text{--}7 \text{ kcal mol}^{-1}$ lower in all cases. Down the group, the metal ion and the donor oxygen atom bond length increases. $\text{Li}^+\text{-O}$, $\text{Na}^+\text{-O}$, and $\text{K}^+\text{-O}$ distances are 1.89, 2.31, and 2.66 \AA , respectively (see Figure 3(a), 4(a), and 4(b)). As the ionic radius of the ions increase down the group, the binding distance between the donor oxygen atoms and the metal ions also increases. Consequently, the electrostatic interactions are decreased and so are the binding energies. Although such periodic trends are similar for alkali-earth metal ions (Be^{2+} , Mg^{2+} , Ca^{2+}), due to increased charge and smaller size of the ions, the binding energies are quite high (\sim six times) compared to the alkali metal ions. Moreover, the overall geometry of the dimer complex after binding has occurred is no longer quasi planar (see Figure 4 (c)–(e)) and the structures are rather puckered. For $\text{Mg}^{2+}\text{-MgC}_6\text{-6C2}$, there is a dative bond between the Mg and O atoms with a Wiberg bond index (WBI)^[58] of 0.0479. For this host, Be^{2+} exhibits the highest binding strength and the values are in the range of -266.88 to $-287.64 \text{ kcal mol}^{-1}$ at different levels (see Table 2).

$\text{M}^{+/2+}\text{-MgC}_6\text{-9C3}$

The trimer host molecule is in a bowl shape with C_{3v} symmetry. For this host as well, two different binding sites have been identified (see Figure 5). However, unlike the dimer, in the case of trimer, both the structures are equally competitive. The smaller ions (Li^+ and Be^{2+}) prefer the structure that exhibits electrostatic and alkene-metal-ion interactions (see Figure 5 (a) and (c)). For Li^+ - and $\text{Be}^{2+}\text{-MgC}_6\text{-9C3}$, these geometries are found to be slightly more stable by 1.20 and 4.33 kcal mol^{-1} , respectively. The other structures (see Figure 5 (b) and (d)) that show electrostatic and alkyne-metal-ion interactions are slightly less stable as the $\text{Li}^+\text{-O}$ (3.81 $^\circ\text{\AA}$) and $\text{Be}^{2+}\text{-O}$ (3.52 $^\circ\text{\AA}$) distances are quite large. This indirectly implies that the electrostatic interactions are weak here though the alkyne-metal-ion interactions are dominant. Therefore, we have calculated all our binding energies for Li^+ - and $\text{Be}^{2+}\text{-MgC}_6\text{-9C3}$ using their most stable structures. However, for Na^+ , K^+ , and $\text{Mg}^{2+}\text{-MgC}_6\text{-9C3}$, where the binding occurs on the side are more stable by 1.29, 0.86, and 8.43 kcal mol^{-1} , respectively. For $\text{Ca}^{2+}\text{-MgC}_6\text{-9C3}$, binding occurring at the center was found to be more stable by 0.76 kcal mol^{-1} . For brevity, these most stable structures alone are shown in Figure 6 and the binding

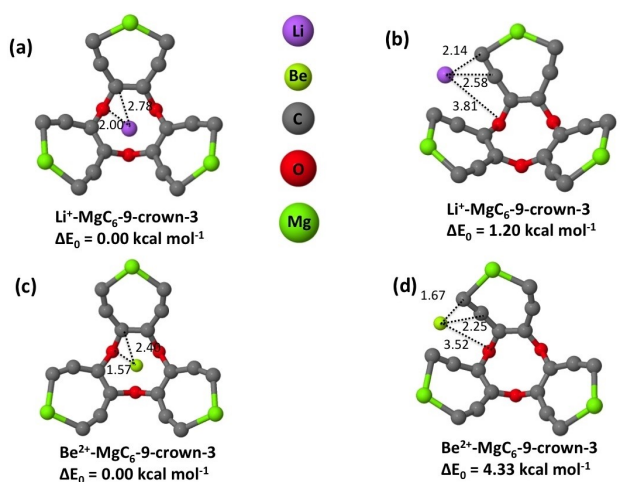


Figure 5. Two different optimized structures of Li^+ - MgC_6 -9C3 ((a) and (b)) and Be^{2+} - MgC_6 -9C3 ((c) and (d)) identified at the B3LYP-D3BJ/6-311++G(2d,2p) level of theory. (a) and (c) – binding occurs at the center; (b) and (d) – binding occurs on the side. Key bond length parameters are given in \AA .

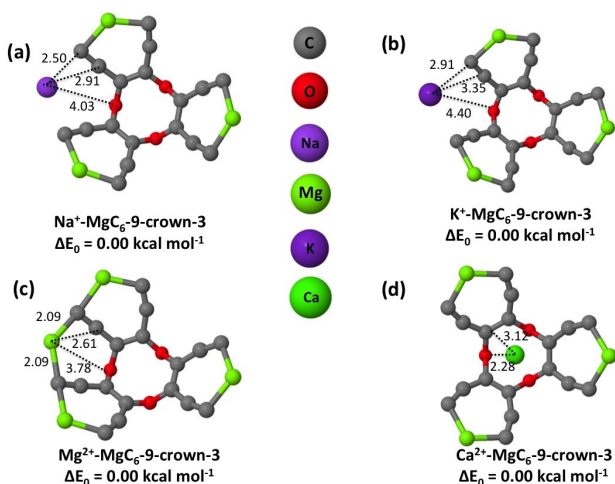


Figure 6. Optimized structures of (a) Na^+ - MgC_6 -9C3; (b) K^+ - MgC_6 -9C3; (c) Mg^{2+} - MgC_6 -9C3; and (d) Ca^{2+} - MgC_6 -9C3 identified at the B3LYP-D3BJ/6-311++G(2d,2p) level of theory. Key bond length parameters are given in \AA .

energy values shown in Table 2 are calculated using these most stable structures at all levels.

The binding energy values calculated for Li^+ are in the range of -63.42 to -68.34 (lowest to highest) kcal mol^{-1} . The values calculated by us at different levels closely matches with one of the trioxane derivatives reported elsewhere at the B3LYP/6-31++G(d,p) level.^[59] Within group 2, the smallest ion Be^{2+} exhibits the highest binding affinity at all levels. The ΔE values are in the range of -337.02 to -355.21 kcal mol^{-1} . The Gibbs free energy values (ΔG) are consistently 7 to 8 kcal mol^{-1} less than the binding energy values for all the six ions. In general, binding affinity within a group (here group 1 and 2) decreases down the group. This periodic trend could be

explained due to the increase in the ionic radii of the ions down a given group. For Mg^{2+} - MgC_6 -9C3, WBI has been calculated at the B3LYP/6-311++G(2d,2p) level of theory. We found that there is a dative bond between the Mg and C atoms (2.09 \AA) with a WBI value of 0.1792, which almost appears like forming a covalent bond bridging the two MgC_6 units (see Figure 6(c)).

$\text{M}^{+/2+}$ - MgC_6 -12C4

Unlike the lower homologues, MgC_6 -6C2 and MgC_6 -9C3, for this system we found two isomers (see Figure 2). The most stable isomer is in S_4 symmetry and the second most isomer forms a bridge between two MgC_6 units. The second isomer, which has a cross-link, is $45.67 \text{ kcal mol}^{-1}$ above the low-lying isomer at the B3LYP-D3BJ/6-311++G(2d,2p) level of theory. The ZPVE-corrected energy gap calculated at the B3LYP/6-311++G(2d,2p), TPSSH/6-311++G(2d,2p), TPSSH-D3BJ/6-311++G(2d,2p), and M06-2X/6-311++G(2d,2p) levels are 35.93, 41.04, 47.70, and $46.72 \text{ kcal mol}^{-1}$, respectively. The energy gap calculated with Grimme's empirical dispersion corrections^[44] involving D3BJ damping^[45,46] or Truhlar's Minnesota functional, M06-2X,^[49] that has certain amount of in-built empirical dispersion corrections are consistently 8–10 kcal mol^{-1} higher, which indirectly indicates that these corrections are key to retrieve accurate energy differences.

Three different binding sites have been identified for the low-lying MgC_6 -12C4 isomer (see Figure 7) with the Li^+ and Be^{2+} ions. Like the dimer host, for the tetramer too, the isomers with both electrostatic and metal-ion-alkyne interactions were found to be the most stable molecules. For Li^+ , the next two isomers are 15.86 and $59.91 \text{ kcal mol}^{-1}$ above the most stable isomer (see Figure 7 (b) and (c)), whereas for Be^{2+} the next two isomers are 0.62 and $50.04 \text{ kcal mol}^{-1}$ (see Figure 7 (e) and (f)), respectively, at the B3LYP-D3BJ/6-311++G(2d,2p) level of theory. Keeping the metal-ion inside the cage, where it can bind with the donor oxygen atoms, seems to be not a viable option as it gives positive or very low binding energy values in all cases. As mentioned above in other cases, the binding energy values have been reported using the most stable structures and they are collected in Table 3.

For Na^+ - and K^+ - MgC_6 -12C4, the structures where the binding occurs on the side with electrostatic and metal-ion-alkyne interactions were found to be the most stable (see Figure 8 (a) and (b)). Their second most stable isomers are by 20.52 and $18.62 \text{ kcal mol}^{-1}$, respectively, above their corresponding most stable isomers. For brevity, these geometries are not shown. Geometry optimizations starting from the least stable geometry (see Figure 7 (c)), where the ion resides inside the cage leads to the most stable geometry in Na^+ - and K^+ - MgC_6 -12C4 cases, which are due to increased ionic radii of the metal ions. Therefore, for larger ions (Na^+ and K^+), we could find only two most stable isomers unlike the Li^+ - or Be^{2+} - MgC_6 -12C4 case. For Mg^{2+} - and Ca^{2+} - MgC_6 -12C4, the most stable isomers are shown in Figure 8 (c) and (d), respectively. Their second most stable isomers are 16.17 and $22.57 \text{ kcal mol}^{-1}$, respectively, above their corresponding most stable isomers.

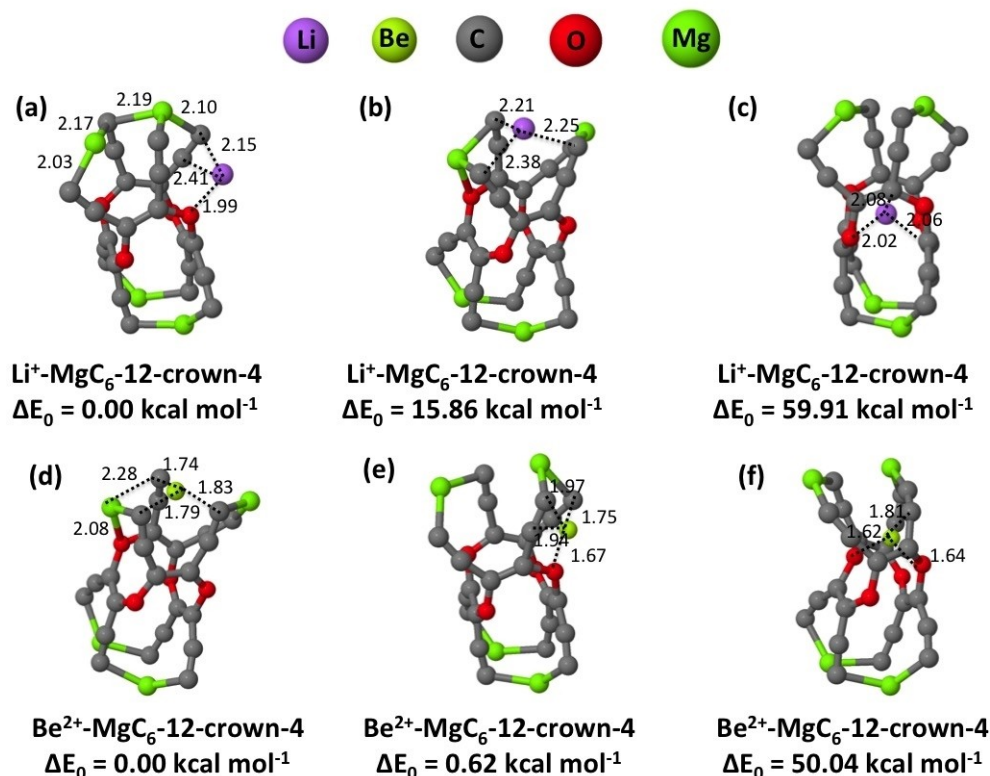


Figure 7. Three different optimized binding sites for Li^+ (a–c) and Be^{2+} (d–f) for the low-lying $\text{MgC}_6\text{-12C4}$ host identified at the B3LYP–D3BJ/6-311 + + G(2d,2p) level of theory. Key bond length parameters are given in Ångstrom.

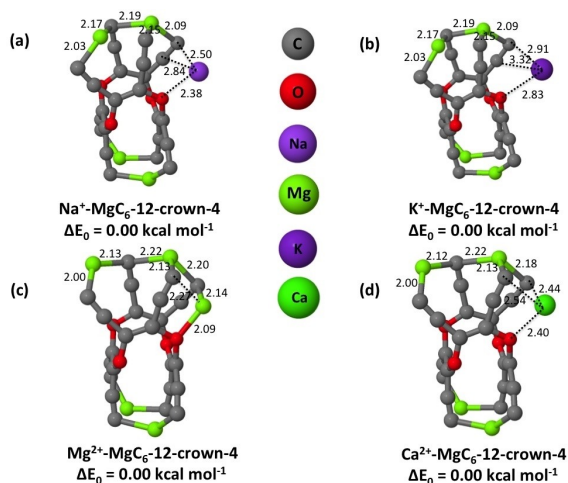


Figure 8. Optimized structures with the low-lying isomer of $\text{MgC}_6\text{-12C4}$: (a) $\text{Na}^+\text{-MgC}_6\text{-12C4}$; (b) $\text{K}^+\text{-MgC}_6\text{-12C4}$; (c) $\text{Mg}^{2+}\text{-MgC}_6\text{-12C4}$; and (d) $\text{Ca}^{2+}\text{-MgC}_6\text{-12C4}$ identified at the B3LYP–D3BJ/6-311 + + G(2d,2p) level of theory. Key bond length parameters are given in Ångstrom.

Quite surprisingly, the binding energies and Gibbs free energies obtained for six different metal ions with the low-lying $\text{MgC}_6\text{-12C4}$ host are less than the values obtained with the lower homologue, $\text{MgC}_6\text{-9C3}$ (see Tables 2 and 3). This trend indirectly indicates that the chances of electrostatic and metal-

ion-alkyne or metal-ion-alkene interactions are ideal with the trimer than the low-lying tetramer. Therefore, for Be^{2+} encapsulation, the trimer will be an ideal host than the low-lying tetramer.

With the high-lying $\text{MgC}_6\text{-12C4}$ host, three and four different binding sites have been identified with the Li^+ (see Figure 9 (a–c)) and Be^{2+} ions (see Figure 9 (d–g)), respectively. Unlike the low-lying isomer, here for Li^+ , the isomer with dominant metal-ion-alkyne interactions alone is the most stable geometry. The second and third isomers for $\text{Li}^+\text{-MgC}_6\text{-12C4}$ are 2.53 and 25.99 kcal mol^{−1}, respectively, above the most stable isomer. For Be^{2+} too, the isomer that exhibits strong metal-ion-alkyne interactions is found to be the most stable molecule. The next three isomers are 16.21, 26.08, and 60.24 kcal mol^{−1} above the most stable geometry, respectively, at the same level. In the second isomer, Be^{2+} forms a tetrahedral kind of motif and rearranges the host molecule like a propeller. We have seen Be^{2+} making such a twisting arrangement with flat crown ether molecules.^[60] It is also noted here that Be atom making tetrahedral tetracoordination is quite usual and reported elsewhere in the literature.^[61–63] For Na^+ and $\text{K}^+\text{-MgC}_6\text{-12C4}$ (high), we could find only two stationary points instead of three as keeping these ions on the side leads to the second most stable isomer. For brevity, only the most stable isomers alone are shown in these cases (see Figure 10). For Na^+ - and $\text{K}^+\text{-MgC}_6\text{-12C4}$ (high), the second most stable isomers are 7.31 and 6.03 kcal mol^{−1}, respectively, above their

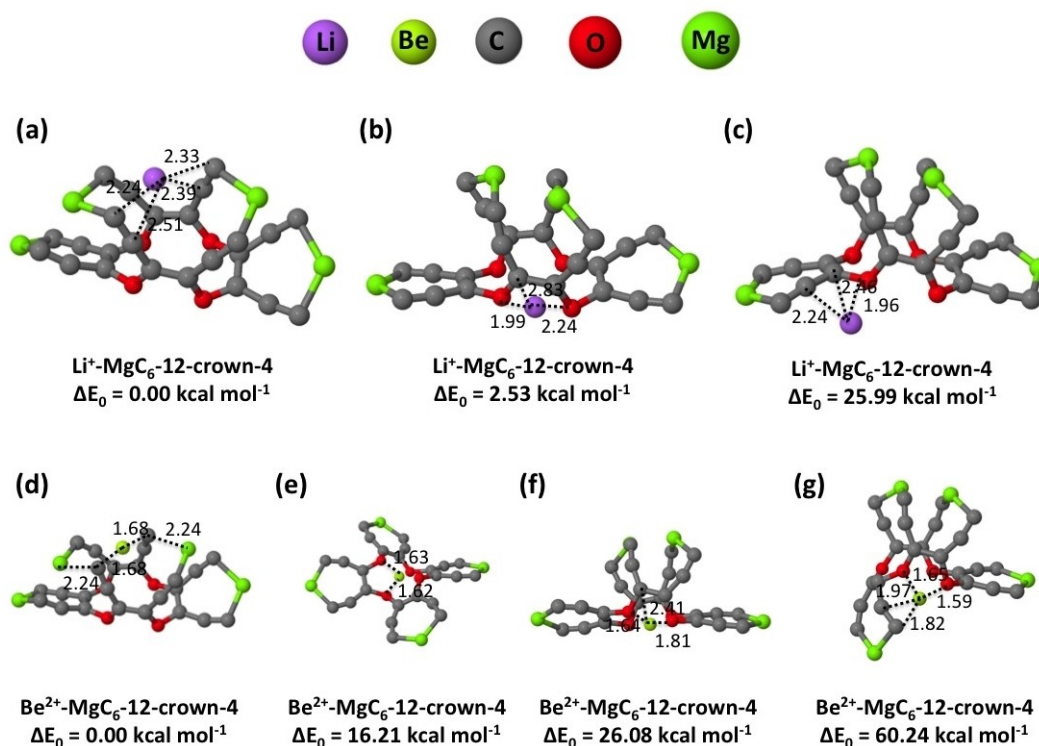


Figure 9. Three and four different optimized binding sites for Li^+ (a–c) and Be^{2+} (d–g), respectively, with the high-lying $\text{MgC}_6\text{-12C4}$ host identified at the B3LYP–D3BJ/6-311 + G(2d,2p) level of theory. Key bond length parameters are given in $^\circ\text{Å}$ ngstrom.

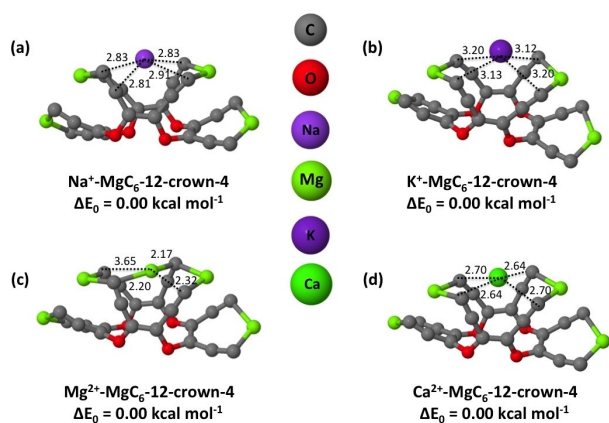


Figure 10. Optimized structures with the high-lying isomer of $\text{MgC}_6\text{-12C4}$: (a) $\text{Na}^+\text{-MgC}_6\text{-12C4}$; (b) $\text{K}^+\text{-MgC}_6\text{-12C4}$; (c) $\text{Mg}^{2+}\text{-MgC}_6\text{-12C4}$; and (d) $\text{Ca}^{2+}\text{-MgC}_6\text{-12C4}$ identified at the B3LYP–D3BJ/6-311 + G(2d,2p) level of theory. Key bond length parameters are given in $^\circ\text{Å}$ ngstrom.

most stable ones. For Mg^{2+} and $\text{Ca}^{2+}\text{-MgC}_6\text{-12C4}$, we could find three different stationary points unlike Na^+ - and K^+ . The second and third most isomers for $\text{Mg}^{2+}\text{-MgC}_6\text{-12C4}$ are 33.79 and 64.83 kcal mol^{-1} above, whereas for $\text{Ca}^{2+}\text{-MgC}_6\text{-12C4}$, the second and third isomers are 33.83 and 60.64 kcal mol^{-1} above their most stable ones. For brevity, we have not shown the high-energy $\text{MgC}_6\text{-12C4}$ isomers for Na^+ , K^+ , Mg^{2+} , and Ca^{2+} .

With the high-lying isomer of $\text{MgC}_6\text{-12C4}$, binding energy values obtained for all the alkaline-earth metal ions (Be^{2+} , Mg^{2+} , and Ca^{2+}) are higher than the $\text{MgC}_6\text{-9C3}$ host. The binding energy values obtained for the alkali metal ions (Li^+ , Na^+ , and K^+) are also slightly higher with the high-energy isomer of $\text{MgC}_6\text{-12C4}$ than with the $\text{MgC}_6\text{-9C3}$ host. The only exception here to this trend are the values obtained at the B3LYP/6-311 + G(2d,2p) level. However, for this study we rely on the values obtained with the empirical dispersion corrections. EDA analyses were also done for all ions with various host molecules. The EDA values from SAPT0 calculations in terms of electrostatic, exchange, induction, and dispersion terms are shown in the supporting information for brevity. These values indicate that the dominant contributions for stabilizing interactions and a higher value of binding energy in the case of Be^{2+} are mostly due to induction. Electrostatic interactions are the second major contributing factor for Be^{2+} .

To confirm the kinetic stability of the host molecules, AIMD simulations have been carried out (see Figure 11) using the ADMP approach^[50] included in Gaussian 16 program.^[51] These simulations have been done for 500 fs at 298 K. We do not see huge fluctuations in energy or structural changes occurring during the entire simulation. Therefore, it is concluded that the host molecules are not only thermodynamically stable but also kinetically stable.

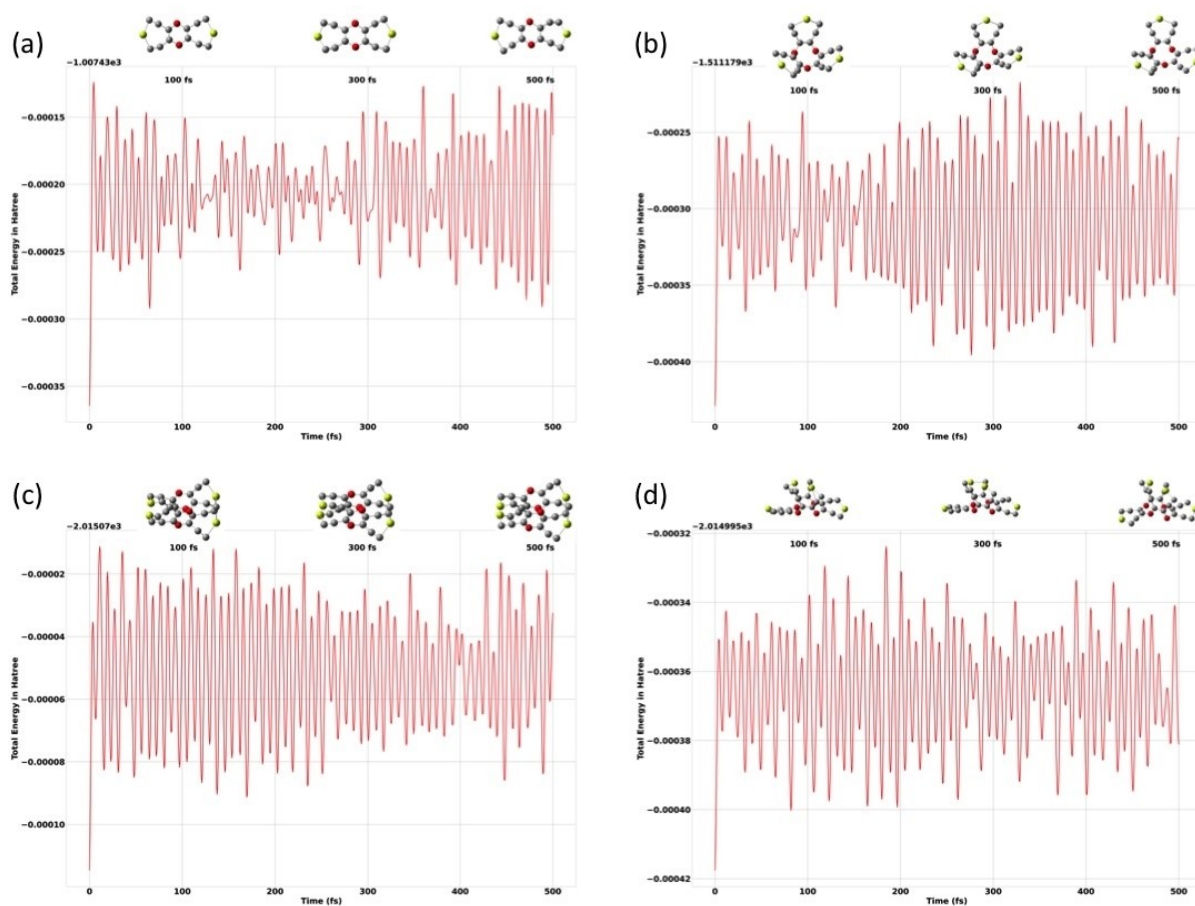


Figure 11. Energy evolution of host molecules (a) MgC_6 -6-crown-2; (b) MgC_6 -9C3; (c) MgC_6 -12C4 (low); (d) MgC_6 -12C4 (high) at 298 K for 500 fs. AIMD simulations have been carried out at the B3LYP/6-31G(d) level of theory.

Conclusions

A brand new series of organomagnesium crown ethers have been theoretically designed using DFT for the first time. Alkali (Li^+ , Na^+ , and K^+) and alkaline-earth metal-ion (Be^{2+} , Mg^{2+} , and Ca^{2+}) chelated crown ethers have been identified. Binding affinities of these ions with organomagnesium crown ether host molecules have been estimated to gauge their binding strengths. Binding energies are calculated at 0 K, whereas the thermally-corrected ZPVE-inclusive Gibbs free energy values are reported at 298.15 K. These values suggest that Li^+ ion has the highest binding affinity among the alkali metal ions whereas Be^{2+} ion shows the highest strength among the alkaline-earth metal ions. Compared to normal crown ether molecules in the literature, it is noted here that the binding affinity of Li^+ ion is low. However, the values are comparable to trioxane derivatives^[59] and dibenzo-14-crown-4 derivatives^[19] reported elsewhere. On the other hand, among the alkaline-earth metal ions, the binding strength of Be^{2+} ion is excessively high. In particular, for Be^{2+} encapsulation, the trimer MgC_6 -9C3 and the high-energy MgC_6 -12C4 seem to be ideal host molecules, which is inferred through higher binding energy values. On the basis of EDA analyses, it is further concluded that induction is the prime reason why these molecules exhibited higher-bind-

ing energy values in the case of Be^{2+} . Through MD simulations, we conclude that these host molecules are kinetically stable.

Supporting Information Summary

Cartesian coordinates of the optimized geometries, total electronic energies, ZPVEs, ZPVE-corrected total energies, number of imaginary frequencies, Free energy correction, Free energy corrected total energies, and EDA values obtained at different levels are given.

Funding Information

This research work carried out here did not receive any specific grant from funding agencies in the public, commercial, or not-for-profit sectors.

Research Resources

Research resources through computational support provided at the SDSU by DURIP Grant W911NF-10-1-0157 from the U.S. Department of Defense and by NSF CRIF Grant CHE-0947087 are gratefully acknowledged. Additional computational support

provided to KT at VIT, Vellore, India, provided through a research grant (Project. No. YSS/2014/001019) from the Science and Engineering Research Board, Department of Science and Technology, New Delhi, Government of India, is also gratefully acknowledged. This work also used the Supercomputing facility of IIT Kharagpur established under National Supercomputing Mission (NSM), Government of India and supported by Centre for Development of Advanced Computing (CDAC), Pune.

Acknowledgments

VST thanks Prof. Andrew L. Cooksy (SDSU), Dr. Ramakrishnan Sethu (Ocugen), and Dr. Kuppuswamy Arumugam (Wright State University) for their interest in this work and useful discussions. We also thank Dr. Ganesh Venkataraman (IIT Kharagpur) for his interest and suggestions on the synthetic viability of these molecules.

Conflict of Interest

The authors declare no conflict of interest.

Keywords: organomagnesium crowns · host-guest molecules · alkali metal ions · alkaline earth metal ions · binding energies · Be²⁺ encapsulation

- [1] R. M. Izatt, J. S. Bradshaw, S. A. Nielsen, J. D. Lamb, J. J. Christensen, D. Sen, *Chem. Rev.* **1985**, *85*, 271–339.
- [2] K. E. Krakowiak, J. S. Bradshaw, D. J. Zamecka-Krakowiak, *Chem. Rev.* **1989**, *89*, 929–972.
- [3] R. M. Izatt, J. S. Bradshaw, K. Pawlak, R. L. Bruening, B. J. Tarbet, *Chem. Rev.* **1992**, *92*, 1261–1354.
- [4] R. M. Izatt, K. Pawlak, J. S. Bradshaw, R. L. Bruening, *Chem. Rev.* **1995**, *95*, 2529–2586.
- [5] M. Stredansky, E. Turco, Z. Feng, R. Costantini, G. Comelli, A. Verdini, L. Flore-ano, A. Morgante, C. Dri, A. Cossaro, *Nanoscale Adv.* **2019**, *1*, 1721–1725.
- [6] C. J. Pedersen, *J. Am. Chem. Soc.* **1967**, *89*, 2495–2496.
- [7] C. J. Pedersen, *Science* **1988**, *241*, 536–540.
- [8] C. Yoo, H. M. Dodge, A. J. M. Miller, *Chem. Commun.* **2019**, *55*, 5047–5059.
- [9] R. Chiarizia, E. P. Horwitz, M. L. Dietz, *Solvent Extr. Ion Exch.* **1992**, *10*, 337–361.
- [10] E. G. Jayasree, C. Sukumar, *Struct. Chem.* **2021**, *1–10* (in press).
- [11] I. A. Shkrob, T. W. Marin, M. L. Dietz, *J. Phys. Chem. B* **2011**, *115*, 3903–3911.
- [12] A. Sengupta, P. K. Mohapatra, *Supramol. Chem.* **2012**, *24*, 771–778.
- [13] Z. Lin, L. Zhongqun, C. Wenjun, C. Shaojin, *J. Radioanal. Nucl. Chem.* **1996**, *205*, 49–56.
- [14] J. W. Grate, R. Strebin, J. Janata, O. Egorov, J. Ruzicka, *Anal. Chem.* **1996**, *68*, 333–340.
- [15] M. B. More, D. Ray, P. B. Armentrout, *J. Am. Chem. Soc.* **1999**, *121*, 417–423.
- [16] E. D. Glendening, D. Feller, M. A. Thompson, *J. Am. Chem. Soc.* **1994**, *116*, 10657–10669.
- [17] D. Feller, *J. Phys. Chem. A* **1997**, *101*, 2723–2731.
- [18] A. van der Ham, T. Hansen, G. Lodder, J. D. C. Codée, T. A. Hamlin, D. V. Filippov, *ChemPhysChem* **2019**, *20*, 2103–2109.
- [19] Y. Tian, W. Chen, Z. Zhao, L. Xu, B. Tong, *J. Mol. Model.* **2020**, *26*, 67.
- [20] K. Thirumoorthy, U. K. Padidela, P. Vairaprakash, V. S. Thimmakonda, *ChemRxiv* **2021**. DOI: 10.26434/chemrxiv.13619378.v1.
- [21] A. P. Pandey, U. K. Padidela, L. K. Thulasiraman, R. Sethu, P. Vairaprakash, V. S. Thimmakonda, *J. Phys. Chem. A* **2020**, *124*, 7518–7525.
- [22] P. Redondo, C. Barrientos, A. Cimas, A. Largo, *J. Phys. Chem. A* **2003**, *107*, 6317–6325.
- [23] D. M. Lowe, P. T. Corbett, P. Murray-Rust, R. C. Glen, *J. Chem. Inf. Model.* **2011**, *51*, 739–753.
- [24] R. Puchta, R. van Eldik, *Z. Anorg. Allg. Chem.* **2008**, *634*, 735–739.
- [25] Y. Ruan, Y. Zhu, Y. Zhang, Q. Gao, X. Lu, L. Lu, *Langmuir* **2016**, *32*, 13778–13786.
- [26] M. R. Buchner, *Chem. Commun.* **2020**, *56*, 8895–8907.
- [27] D. J. Nixon, L. C. Perera, T. N. Dais, P. J. Brothers, W. Henderson, P. G. Plieger, *Phys. Chem. Chem. Phys.* **2019**, *21*, 19660–19666.
- [28] Y. A. Ermakov, K. Kamaraju, A. Dunina-Barkovskaya, K. S. Vishnyakova, Y. E. Yegorov, A. Anishkin, S. Sukharev, *Biochemistry* **2017**, *56*, 5457–5470.
- [29] S. De, G. Sabu, M. Zacharias, *Phys. Chem. Chem. Phys.* **2020**, *22*, 799–810.
- [30] A. N. Leonard, J. B. Klauda, S. Sukharev, *J. Phys. Chem. B* **2019**, *123*, 1554–1565.
- [31] D. Naglav, M. R. Buchner, G. Bendt, F. Kraus, S. Schulz, *Angew. Chem. Int. Ed.* **2016**, *55*, 10562–10576; *Angew. Chem.* **2016**, *128*, 10718–10733.
- [32] L. C. Perera, O. Raymond, W. Henderson, P. J. Brothers, P. G. Plieger, *Coord. Chem. Rev.* **2017**, *352*, 264–290.
- [33] M. R. Buchner, *Chem. Eur. J.* **2019**, *25*, 12018–12036.
- [34] B. Neumu"ller, K. Dehnicke, *Z. Anorg. Allg. Chem.* **2006**, *632*, 1681–1686.
- [35] R. Puchta, R. Kolbig, F. Weller, B. Neumu"ller, W. Massa, K. Dehnicke, *Z. Anorg. Allg. Chem.* **2010**, *636*, 2364–2371.
- [36] B. Neumu"ller, K. Dehnicke, R. Puchta, *Z. Anorg. Allg. Chem.* **2008**, *634*, 1473–1476.
- [37] M. R. Buchner, M. Mu"ller, *Z. Anorg. Allg. Chem.* **2018**, *644*, 1186–1189.
- [38] M. Mu"ller, M. R. Buchner, *Chem. Eur. J.* **2020**, *26*, 9915–9922.
- [39] C. Lee, W. Yang, R. G. Parr, *Phys. Rev. B* **1988**, *37*, 785–789.
- [40] A. D. Becke, *Phys. Rev. A* **1988**, *38*, 3098–3100.
- [41] A. D. Becke, *J. Chem. Phys.* **1993**, *98*, 5648–5652.
- [42] R. Krishnan, J. S. Binkley, R. Seeger, J. A. Pople, *J. Chem. Phys.* **1980**, *72*, 650–654.
- [43] T. Clark, J. Chandrasekhar, G. W. Spitznagel, P. V. R. Schleyer, *J. Comput. Chem.* **1983**, *4*, 294–301.
- [44] S. Grimme, J. Antony, S. Ehrlich, H. Krieg, *J. Chem. Phys.* **2010**, *132*, 154104.
- [45] A. D. Becke, E. R. Johnson, *J. Chem. Phys.* **2005**, *122*, 154104.
- [46] S. Grimme, S. Ehrlich, L. Goerigk, *J. Comput. Chem.* **2011**, *32*, 1456–1465.
- [47] S. Grimme, *WIREs Comput. Mol. Sci.* **2011**, *1*, 211–228.
- [48] J. Tao, J. P. Perdew, V. N. Staroverov, G. E. Scuseria, *Phys. Rev. Lett.* **2003**, *91*, 146401.
- [49] Y. Zhao, D. G. Truhlar, *Theor. Chem. Acc.* **2008**, *120*, 215–241.
- [50] H. B. Schlegel, J. M. Millam, S. S. Iyengar, G. A. Voth, A. D. Daniels, G. E. Scuseria, M. J. Frisch, *J. Chem. Phys.* **2001**, *114*, 9758–9763.
- [51] M. J. Frisch, et al. Gaussian 16 Revision B.01. 2016; Gaussian Inc. Wallingford CT.
- [52] M. J. S. Phipps, T. Fox, C. S. Tautermann, C.-K. Skylaris, *Chem. Soc. Rev.* **2015**, *44*, 3177–3211.
- [53] B. Jeziorski, R. Moszynski, K. Szalewicz, *Chem. Rev.* **1994**, *94*, 1887–1930.
- [54] D. G. A. Smith, *J. Chem. Phys.* **2020**, *152*, 184108.
- [55] E. G. Hohenstein, C. D. Sherrill, *J. Chem. Phys.* **2010**, *132*, 184111.
- [56] E. G. Hohenstein, R. M. Parrish, C. D. Sherrill, J. M. Turney, H. F. Schaefer, *J. Chem. Phys.* **2011**, *135*, 174107.
- [57] F. Weigend, R. Ahlrichs, *Phys. Chem. Chem. Phys.* **2005**, *7*, 3297–3305.
- [58] E. D. Glendening, F. Weinhold, *J. Comput. Chem.* **1998**, *19*, 593–609.
- [59] S. J. Cho, *Bull. Korean Chem. Soc.* **2014**, *35*, 2723–2725.
- [60] K. Thirumoorthy, V. S. Thimmakonda, *Int. J. Quantum Chem.* **2021**, *121*, e26479.
- [61] M. R. Buchner, M. Müller, N. Spang, *Dalton Trans.* **2020**, *49*, 7708–7712.
- [62] M. R. Buchner, M. Müller, F. Dankert, K. Reuter, C. von H"anisch, *Dalton Trans.* **2018**, *47*, 16393–16397.
- [63] M. Mu"ller, M. R. Buchner, *Chem. Eur. J.* **2019**, *25*, 16257–16269.

Submitted: July 2, 2021

Accepted: August 23, 2021